ROYAL SOCIETY OF CHEMISTRY

COMMUNICATION

Check for updates

Detection of Br and I as atomic anions using liquid sampling – atmospheric pressure glow discharge/Orbitrap mass spectrometry

Dehlia A. Lang, [ID] [a] Joseph V. Goodwin, [ID] [a] Cameron J. Stouffer, [ID] [a] Benjamin T. Manard [ID] [b] and R. Kenneth Marcus [ID] *[a]

The quantification and determination of halogen isotope composition is essential in many fields including geochemistry and nuclear forensics. Detection of the halogen elements is commonly attempted with inductively coupled plasma mass spectrometry (ICP-MS) however, there are multiple challenges faced. Most significantly this includes very poor ionization efficiency and the potential for isobaric interferences from either matrix or plasma species. Thus, sensitivity and accuracy are often limiting issues. Here a liquid sampling-atmospheric pressure glow discharge (LS-APGD) ionization source is coupled with an ultrahigh resolution Orbitrap MS to perform halogen detection of bromine and iodine as initial analytes. This facilitates simple and sensitive detection of these elements as atomic anions from simple aqueous salt solutions. Collision-induced dissociation (CID) and higher-energy collisional dissociation (HCD) energies were optimized to produce the maximum response of Br^- and I^-. The LS-APGD conditions were optimized using a design of experiments (DOE) approach for Br^- and I^- concurrently. Response curves for Br^- and I^- solutions determined limit of detection (LOD) values of 50 pg and 5 pg, respectively, in 20 μL aliquots. The curves indicated response factors of 0.67 for $^{79}Br^-$ and 0.90 for $^{127}I^-$. Br isotope ratios were determined with precision between 0.7 and 7.3% RSD, with the isotope ratios determined with precision 0.8% RSD at concentrations above the limit of quantification. Preliminary tests were conducted to evaluate the effect of different cations (Na^+, K^+, and Mg^{2+}) on Br^- responses, with no discernible impacts observed on the halogen signal responses. This study demonstrates the potential use of the LS-APGD-Orbitrap-MS for the detection of multiple halogens while avoiding interferences, minimizing sample preparation, and overcoming ionization barriers.

Introduction

Halogens can serve as indicators across diverse fields ranging from geochemical,[1] environmental,[2,3] biological,[4] and nuclear

forensics[5] analysis. The ability to simultaneously measure bromine (Br) and iodine (I) is particularly valuable, as it aids in halogen resource tracking and sheds light on unique geochemical processes, such as phase separation in ore-forming fluids.[6] In biological applications, halogen detection provides benefits in areas such as dentistry where fluoride is used for teeth protection.[7] In the environmental arena, the accurate determination of per- and polyfluoroalkyl substances (PFAS) which have been a topic of concern by virtue of their high bioaccumulation rate and persistence within the environment.[8] Similarly, halogen information is particularly crucial in nuclear forensics, where the Br and I content in uranium ore concentrates (UOC) can reveal important insights into the production method and the geographic origin of the ore.[9] Understanding the halogen content in UOC plays a critical role in assessing whether the material complies with nuclear-grade specifications, evaluating facility designs, tracing material origins, and even detecting potential material substitutions,[10] clearly, high quality methods for the determination of bromine and iodine are of great relevance.

The current state of the field of halogen analyses involves methods that generally require lengthy and complicated sample preparation processes which often cause issues with the analysis such as analyte loss and contamination, or are simply of insufficient sensitivity.[11] Analyses using atomic spectrometric methods such as ICP-MS/OES perhaps require extensive sample preparation procedures[12] such as acid digestion which leads to analyte loss due to the formation of volatile halogen acid vapors.[2,13] Matrix effects, interferences, and ionization enhancement/suppression can also occur if incompatible solvents are used.[14] Ultimately, by virtue of having relatively high ionization potentials, the halogens exhibit comparatively low ionization efficiencies in the plasma *versus* metals, leading to relatively poor limits of detection (LODs). This is frequently seen in the analysis of iodine using ICP-MS, since the first ionization potential is at a value of 10.35 eV and can cause inefficient ionization of iodine or even the absence of complete ionization leading insufficient LOD values.[15] For example, while

[a]Department of Chemistry, Clemson University, Clemson, SC 29634, USA. E-mail: marcusr@clemson.edu

[b]Chemical Sciences Division, Oak Ridge National Laboratory, Oak Ridge, TN 37831, USA

This journal is © The Royal Society of Chemistry 2025

J. Anal. At. Spectrom., 2025, 40, 2625–2632 | **2625**

LODs for transition metals might lie in the range of 0.1–10 pg mL^{-1} in water depending on the metal being analyzed and the MS platform,[16] corresponding instrument detection limit (IDL) values for bromide and iodide anions range between 30–230 pg mL^{-1} and 5–50 pg mL^{-1}, respectively across various MS platforms.[9,14,17,18] Ultimately, the combination of low ionization efficiency, sample preparation complexities, and matrix/isobaric interference mean that the method detection limit (MDL) values are often insufficient for certain applications.[10,14] Therefore, the development of methods with lower detection limits for halogens are crucial for enhancing the ability to detect these trace elements within samples. One example of such approaches is the recent utilization of Ba^{2+} addition to test samples to yield BaF^+ complexes in ICP-MS spectra.[4,19]

The liquid sampling atmospheric pressure glow discharge (LS-APGD) microplasma ionization source, developed by Marcus *et al.*, has proven to provide accurate and sensitive analytical analysis across a broad range of materials, when paired with MS and OES systems.[20] The versatile ionization source requires no modifications to commercial 'organic' MS systems, coupling in place of a standard electrospray ionization (ESI) source, for example.[20–22] It has demonstrated success in ionizing both inorganic and organic compounds and delivering high-quality atomic and molecular mass spectra.[20,23–25] Notably, it functions efficiently under significantly lower operational demands in comparison to conventional ICP applications,[26,27] including relatively low gas flow rates (0.5 L min^{-1} He), much lower applied powers (<60 W), and a solution delivery rate (50 µL min^{-1}). Helium is used as the support gas in the microplasma principally because of its high thermal conductivity, though it may have certain advantages over Ar, for example, in terms of the ionization of the halogens. The ability to operate under these lower energy conditions offers a cost-effective alternative for a wide variety of analytes and allows the direct coupling to conventional ESI-MS instruments, most specifically Orbitrap platforms.[28–30] A key feature in this coupling includes the ability to obtain ultrahigh mass resolution ($m/\Delta m$ of up to 1 000 000), thus alleviating all forms of isobaric interferences encountered to date, where needed.[31–33] The applications of this coupling have rapidly expanded, showcasing its effectiveness in diverse fields such as environmental analysis[25,34] and nuclear forensics.[32,35,36] This study presents initial investigations into the use of the LS-APGD/Orbitrap coupling for detection of bromide and iodide atomic anions towards elemental and isotopic analysis. Opportunities for enhanced MDL performance are seen in the ability to alleviate isobaric interferences *via* ultrahigh mass resolution and the fact that alternative ionization mechanisms may exist *versus* the ICP. It is believed that the approach offers the potential for sensitive determination of these two elements, and sheds light into paths forward in the determination of the other halogens.

Materials and methods

Chemicals and reagents

Solutions for analysis were prepared using analytical-grade NaI (Thermo Fisher Scientific, Waltham, MA, USA), NaBr (Honeywell, Charlotte, NC, USA), KI (Thermo Fisher Scientific, Waltham, MA, USA), and KBr (Thermo Fisher Scientific, Waltham, MA, USA) and deionized water from an Elga PURELAB flex 18.2 MΩ water purification system (Veolia Water Technologies, High Wycombe, England). Each individual salt was made into an aqueous stock solution at a concentration of 10 µg mL^{-1}.

LS-APGD Orbitrap mass spectrometry

A single-electrode liquid sampling-atmospheric pressure glow discharge (LS-APGD) microplasma ionization source was used throughout the experiments (Fig. 1).[37] The source is mounted to the Thermo Scientific Q Exactive Focus Orbitrap (Thermo Scientific, Waltham, MA) mass spectrometer with no modifications to the MS system. All of the mass spectra reported here were acquired in the negative ion mode. The LS-APGD ionization source has a central electrode with an outer stainless-steel tube (0.04 in ID, 1/16 in OD; McMaster Carr, Elmhurst, IL, USA) which directs a sheath gas of helium to the microplasma and an interior silica capillary (250 µm ID, 360 µm OD; Molex, Lisle, IL, USA) that delivers the 2% HNO_3 electrolyte carrier solution as well the 20 µL injection of the aqueous salt test solutions. A single stainless-steel electrode (0.05 in dia. weldable feedthrough, MDC Vacuum Products, LLC, Hayward, CA, USA) is bent to a position 90° perpendicular to the solution electrode. The microplasma is formed and sustained in the 0.5 mm space between the two electrodes. The bent electrode acts as the anode with a high voltage applied while the solution electrode is held at ground potential and acts as the cathode. Discharge current, solution flow, and sheath gas flow rates are controlled by a custom control box (GAA Custom Electronics, Kennewick, WA, USA). The optimization of the plasma conditions was performed using a design-of-experiment (DOE) approach analyzed
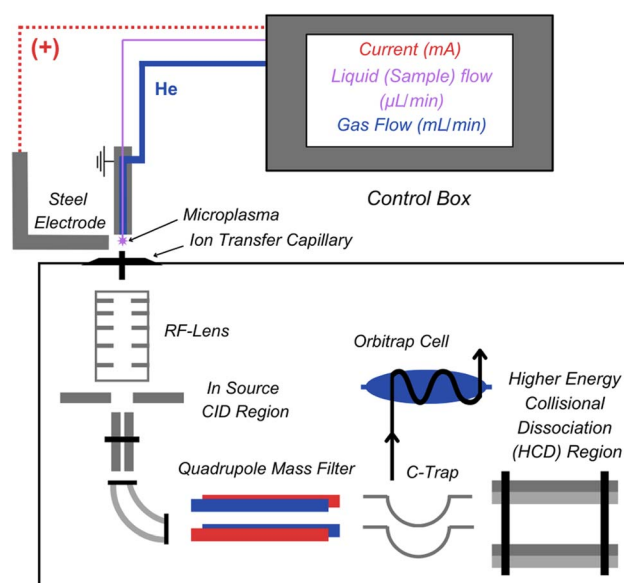

Fig. 1 Diagrammatic representation of the LS-APGD/Orbitrap-MS system using a single-electrode configuration.

using JMP software. The optimized plasma conditions included a solution flow rate of 60 μL min⁻¹, a sheath gas flow rate of 600 mL min⁻¹, and a direct current of 60 mA.

FTMS Booster X2T data acquisition system

The FTMS Booster X2 from Spectroswiss (Lausanne, Switzerland) enhances the Orbitrap's detection system by connecting directly to its pre-amplifier for data acquisition and processing. It works alongside the OEM software of the Orbitrap system and Spectroswiss Peak-by-Peak software.[38] The FTMS Booster improves performance by performing absorption mode Fourier-transforms (aFT), unlike the Orbitrap's enhanced Fourier-transforms (eFT) which only capture positive noise. The aFT processing captures both positive and negative fluctuations, therefore reducing background noise and improving analyte sensitivity.[39] Additionally, the FTMS Booster increases mass resolution by collecting extended ion transients through a "dummy" scan, where ions are stored in the C-trap while a second ion packet is analyzed within the Orbitrap cell.[38–40] This leads to higher resolution without impacting the duty cycle, as the transients collected during the dummy scan are discarded and the analytically relevant signal from the extended transients are processed using the FTMS Booster software. This system has proven invaluable in the microplasma/Orbitrap coupling towards elemental/isotopic analyses by providing higher resolution, analytical sensitivity, and isotope ratio measurement precision.[30,41]

Results and discussion

Initial efforts into the potential use of the LS-APGD microplasma as an ionization source for the analysis of the halogens bromine and iodine involved a direct approach to determine the raw spectral characteristics/composition and the utilization of the collisional-dissociation available on the Orbitrap instrument to simplify those spectra. Initial characterization involved an evaluation of the discharge conditions to achieve optimum halide ion responses and a preliminary evaluation of the system sensitivity. Finally, experiments were performed to gain preliminary insights into the practical operation of the source, with an eye towards isotope ratio determinations.

Spectral characterization and optimization of collisional dissociation conditions

Consistent across applications of the LS-APGD to the analysis of metallic elements is the creation of a diversity of ionic species involving metals complexed with water molecules, hydronium ions, and acid-related counter ions, with metal oxides often lying at the core.[21,42] Aqueous halogen salt solutions present a unique set of challenges as ions containing the halide salt's counter cation (e.g., Na) are also present. The presence of molecular ions containing the target analytes minimize the yields for the target atomic anions in the mass spectrum. A primary motivation described herein is to generate mass spectra composed of the atomic bromine and iodine signals without the interference of extraneous species through the use

of in-source collision-induced dissociation (CID) and higher energy collisional dissociation (HCD),[30] an approach common to metals determination on the LS-APGD/Orbitrap platform.

The native/raw mass spectra obtained for the introduction of NaBr and NaI test solutions are presented in Fig. 2a and b, respectively. (Note, Orbitrap detection/output is not in absolute units of ion current or charge.) It must be reiterated that these spectra are taken in the negative ion mode, and in fact no cationic species related to Br or I are seen in the positive ion mode. In the spectra without any form of collisional dissociation applied there are numerous oxide and water cluster species containing bromine and iodine, primarily BrO, BrO_2, and BrO_3 for bromine and IO, IO_2, and IO_3 for iodine, that lead to decreased intensities for elemental peaks. While halogen oxides are a bit more prevalent for I, in both cases the vast majority of the higher-mass molecular ions involve solvent species, predominantly water-related clusters. Applying in-source CID involves applying a potential difference between the exit of the ion transfer capillary (ITC) and the entrance of the S-lens, wherein energetic collisions occur with background (ambient) gases. Beyond this, HCD collisional dissociation is affected in a rf-only hexapole device wherein the radio frequency (rf) voltage affects the degree of dissociation. Previous studies on metal analytes have shown that the CID process is most effective at reducing the extent of solvent-related background ions, whereas HCD tends to be more effective at reducing species composed of the metal coordinated with an oxygen atom(s) and associated anionic solvent species.[30] As a general rule, the spectra of transition metals exist as monoatomic cations, those of lanthanides as monoxide cations, and actinides as dioxide cations.

To optimize the CID process, the stock NaBr and NaI samples were tested across a range of energies, from 0 eV to 100 eV in 20 eV intervals with measurements involving triplicate 20 μL injections of each. No HCD processing is applied in this experiment. The resulting intensity values (as a percentage of the case of no CID) are plotted for the atomic halogen ions versus the applied CID energies in Fig. 3a. As seen in the figure, the atomic ion signals for both halogens show an initial positive response as the energy is increased up to a potential of 40 volts. Beyond this point, the responses for each show a steady decline as those energies inflict greater amounts of scattering losses from the ion beam. This response to increases in collisional energy is entirely consistent with previous studies of metallic element analytes.[42] Across the full range of CID energies, the triplicate reproducibility for the CID optimization measurements were between 4 and 16% RSD, with both values at the optimal 40 eV energy being 6.3% RSD. The optimization of the HCD process followed a similar methodology, spanning from 0 eV to 100 eV in 20 eV intervals. In this case, the determined optimal CID energy of 40 eV was maintained throughout the study. The resulting intensity plots (Fig. 3b) demonstrate that the most significant increase in signal intensity for both $^{79}Br^-$ and $^{127}I^-$ occurred at an energy of 20 eV, with the observed trends again being consistent with previous efforts.[42] While the relative response improvement for Br^- is appreciable at ~50%, the ~280% improvement for I^- implies that iodine had formed

This journal is © The Royal Society of Chemistry 2025
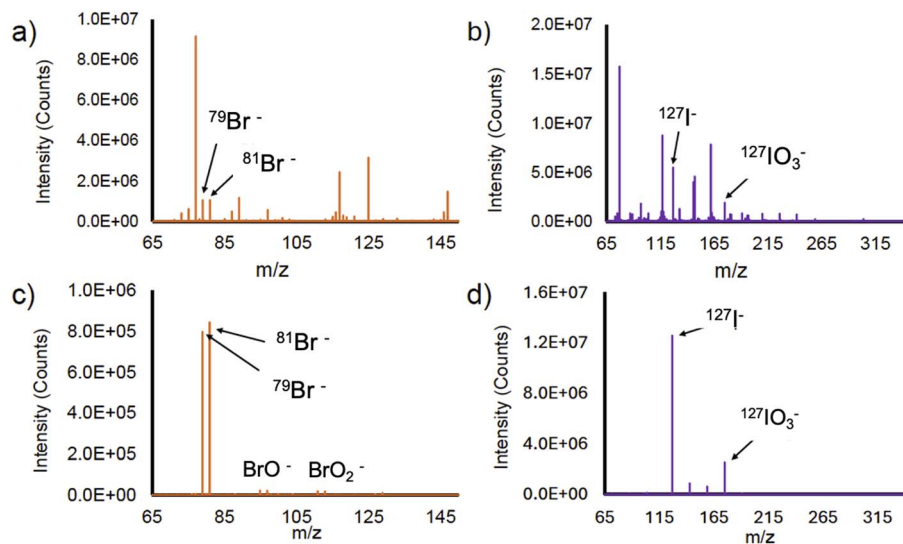
J. Anal. At. Spectrom., 2025, 40, 2625–2632 | 2627

Fig. 2 Mass spectra derived from 20 μL injections of 10 μg mL^{-1} halogen solutions illustrating the use of collisional dissociation. (a) NaBr, no CID, no HCD, (b) NaI, no CID, no HCD, (c) NaBr, CID = 40 eV, HCD = 20 eV and (d) NaI, CID = 40 eV, HCD = 20 eV. Discharge conditions: current = 60 mA, solution flow rate = 60 μL min^{-1}, gas flow rate = 600 mL min^{-1}.

a greater proportion of molecular ion species (*e.g.* oxygenated ions). At the optimal value of 20 eV the precision was 14.4% RSD. It is interesting to note that analogous studies of metal analyte species require HCD energy values of >100 eV for optimum analyte ion yields,[32,35,42] perhaps reflecting greater attractive forces in the case of the cationic species.

As seen in Fig. 2c and d, this systematic optimization of both CID and HCD energies enabled the efficient reduction of interferences, allowing for clear and precise detection of atomic bromine and iodine signals. The remaining ionic species in the spectra reflect the case wherein there are chemical propensities for both halide ions to coordinate with oxygen atoms, where not surprisingly, the thermodynamically stable IO_3^- (iodate) species is still prominent. Table 1 better presents the results of the combined CID processes for the monoatomic halogen anions and their oxyanions. Surprisingly, the production of monoatomic anions, while pronounced, is not as extensive as

the oxyanions. Indeed, the data suggests that, somewhat consistent with the metal cations, the HCD is effective at removing solvent-related species, but not dissociating the oxides themselves. These halogen–oxygen species, existing across a range of neutrals, radicals, and anions, are well known in the inorganic chemistry literature.[43] The creation/dissociation of these species poses some fascinating questions to be investigated in the future. While it might be desirable to further reduce those oxides to the atomic halogen anion form, the data in Fig. 3b suggest that it would be a case of diminishing returns relative to collisional losses of the atomic ions.

Optimization of LS-APGD operating conditions

To achieve optimal signal with high analytical precision and accuracy for the novel case of atomic halide determinations, optimization of the LS-APGD microplasma operation parameters is essential. While it has been found that operation
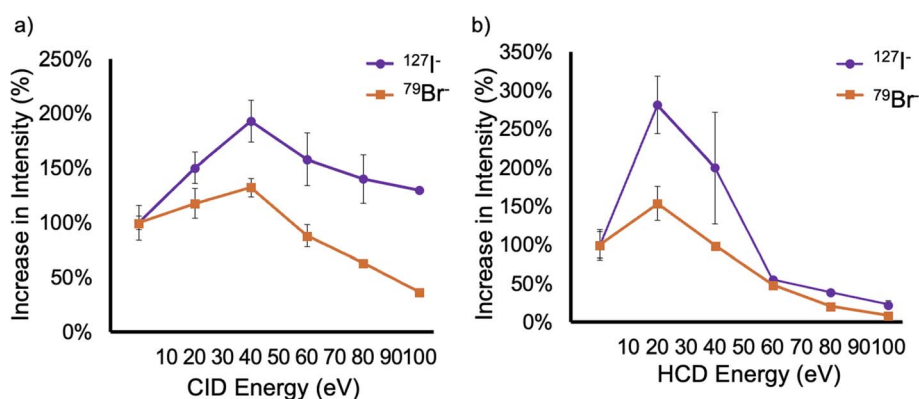

Fig. 3 Relative responses of atomic bromine and iodine ions as a function of increases in (a) CID energy (no HCD employed) and (b) HCD energy with a CID energy value of 40 eV. Discharge conditions: current = 60 mA, solution flow rate = 60 μL min^{-1}, gas flow rate = 600 mL min^{-1}.

Table 1 Relative intensities of halogen related ions without any form of collision-induced dissociation (CID) and with the use of the optimized CID conditions

	$^{79}Br^-$	$^{79}BrO^-$	$^{79}BrO_2^-$	$^{127}I^-$	$^{127}IO^-$	$^{127}IO_2^-$	$^{127}IO_3^-$
No dissociation	1.2×10^5	1.1×10^4	1.5×10^3	4.8×10^6	3.1×10^5	8.9×10^4	1.3×10^4
Dissociation (CID = 40 eV, HCD = 20 eV)	8.0×10^5	1.8×10^4	1.5×10^4	1.4×10^7	3.6×10^6	2.1×10^5	3.8×10^6
Relative increase	$6.7\times$	$16\times$	$10\times$	$2.9\times$	$9.7\times$	$2.4\times$	$290\times$

conditions for the generation of analytically relevant ions across a range of metallic elements are fairly uniform, there is no reason to believe that the same conditions are at all relevant for the halides. Several techniques are available to assess optimal conditions, such as the one-variable-at-a-time (OVAT) method or a design of experiment (DOE) approach. The LS-APGD source in the single electrode configuration has five parameters to consider: discharge current, sheath gas (He) flow rate, solution flow rate, electrode gap, and the distance between the plasma and the entrance to the MS (*i.e.* ion transfer capillary (ITC)). The DOE used in this study is custom design, which is built on D-optimal design, where the user can select and test factors and discrete levels with the best set of experimental runs for estimating a statistical model. The DOE approach employed the JMP Pro® software (JMP Statistical Discovery LLC, Cary, NC, USA) to streamline the optimization process.[36,44] The use of a DOE with JMP generates a carefully selected set of parameter combinations, representing all possible variations without requiring an exhaustive number of experiments, therefore significantly decreasing the required analysis time. Additionally, the model allows for the application of specific numerical levels for each parameter to avoid extreme, unrealistic settings, such as combinations of high currents (>60 mA) and low gas flow rates (<0.1 L min^{-1}), which were based on previous experiences.

Conditions were assessed across a range of 20–60 mA for current, 200–600 mL min^{-1} for gas flow, 10–60 µL min^{-1} for solution flow, 0.5–2 mm for interelectrode gap, and 25–50 mm for distance between plasma and ITC. The resulting $^{79}Br^-$ and $^{127}I^-$ intensity values for different parameters and parameter pairs were compared using a logworth plot within the program

(Fig. 4). The logworth plot is an effective tool for visualizing the significance of each factor: the *p*-values for each parameter or parameter pair are compared, with higher logworth values indicating stronger effects on the plasma's performance. In the analysis, *p*-values below 1.3 ($p \le 0.05$) were excluded, as these suggested that certain parameters had negligible effects on plasma performance. Optimal plasma conditions were found to be a current of 60 mA, solution flow rate of 60 µL min^{-1}, gas flow rate of 600 mL min^{-1}, interelectrode gap of 0.5 mm, and a distance between the plasma and the ITC of 25 mm. The values found showed some similarities and differences to results from DOEs performed on metallic species. High solution and gas flow rates reflected similar results to the analysis of NdO species but the distance to the ITC and electrode gap values differed which could be attributed to the use of a single electrode configuration as compared to the dual electrode.[44] On the other hand, when compared to DOE results from the analysis of Pu species flow rates for both solution and sheath gas were much lower than the optimal conditions for Br and I analysis and distance from ITC was much higher.[35]

Preliminary assessment of analytical characteristics

While much work remains in terms of understanding the operational aspects of the LS-APGD/Orbitrap coupling with regards to atomic halide ion determinations, it is instructive at this point to begin probing some of the application space of the approach. A preliminary assessment of the calibration quality and sensitivity of the method was investigated. Response curves for bromine and iodine were generated separately using NaBr and NaI salt solutions under the standard data acquisition conditions (*i.e.*, not tailored for highest precision and sensitivity) with the integrated areas of the injection transients used as the quantitative measure. For bromine, the response function of $^{79}Br^-$ was generated across a 20 µL injection mass of range of 4.8 to 143.4 ng NaBr (230–7170 ng mL^{-1}), yielding an R^2 value of 0.993 which reflects a linear relationship between signal and injected analyte mass. This response yielded a limit of detection (LOD = $m/3\sigma_{bkg}$) for bromine of 50 pg in 20 µL (2.5 ng mL^{-1}). For iodine, the response curve was generated with an injection mass range of 4.4 to 174.5 ng NaI, with an R^2 value of 0.966 and a much lower LOD of 5 pg of iodine in 20 µL (0.25 ng mL^{-1}). The difference here is due in part to the ~50% higher sensitivity factor in the I$^-$ response curve as well as the fact that I is monoisotopic in comparison to Br. The LOD for iodide is similar to values found in Nd detection and bromide limits of detections were significantly higher than the same Nd studies with a LOD of 5.7 pg across all Nd isotopes.[44] When compared to
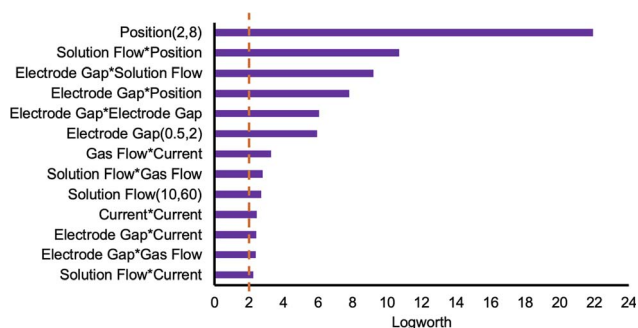

Fig. 4 Pareto plot representing bromide and iodide intensity responses across plasma conditions contained in design of experiment procedure. High logworth values indicate low *p* values and exemplify highly significant effects on the plasma performance. All logworth values below 1.3 were removed for simplicity.

ICP-MS, the LODs achieved here are very similar (within 10%, relative) to previously cited values,[9,14,17,18] without the use of extended Orbitrap FT transient acquisitions, *etc.*

One of the key application areas of the microplasma/ Orbitrap instrument is in the field of isotope ratio mass spectrometry (IRMS).[22,36,44] Previous efforts have demonstrated IR precision of the order of 0.05% RSD for $^{235}U/^{238}U$ determinations having an absolute value of 0.00076.[30] An initial characterization of the IR performance for Br determinations was undertaken of these ratios is of relevance in applications such as environmental sciences where isotopic ratio analysis can be used to monitor the sources and behavior of brominated organic compounds such as polybrominated diphenyl ethers (PDBE).[45] Additionally, bromine isotope ratios can indicate the migration of natural waters in aquifers and different subsurface environments.[46] To gain a preliminary insight into the obtainable IR precision for bromine, triplicate 20 μL injections were performed spanning a bromine solute mass range of 0.019 to 191.2 ng, a concentration range covering 5 orders of magnitude; 0.1–10 000 ng mL^{-1}. As an example of the data format, Fig. 5 presents the extracted ion signal transients for the $^{79}Br^-$ isotope responses for an injected mass of 2 ng Br, yielding a precision of 1.6% RSD for the integrated areas. The obtained isotope ratio data across the bromine mass injection range is presented in Fig. 6. Not surprisingly, both the IR precision and accuracy improve with the mass of injected solute. Notably for the two lowest concentrations, which were both within 10× of the determined bromine LOD, the percentage relative standard deviation (% RSD) values were the highest at 9.1 and 13.6%, with the scatter and perhaps lower absolute values likely affected by contributions from spectral noise. For those solutions having Br$^-$ concentrations over 1 ng mL^{-1}, triplicate 20 μL injections yielded precision values between 0.7 and 7.5% RSD, with an average $^{79}Br/^{81}Br$ value of 0.992 *versus* the accepted, natural $^{79}Br/^{81}Br$ IR value of 1.0279.[47] In this case, the obtained IR value deviates only 3.5% from the accepted value; without any mass bias correction. Regarding precision, at the 10 ng mL^{-1} level a ratio variability of 0.8% RSD was obtained for triplicate injections, a value in line with the precision found for the $^{142}Nd/^{144}Nd$ precision of 0.3% RSD,[44] acquired under the
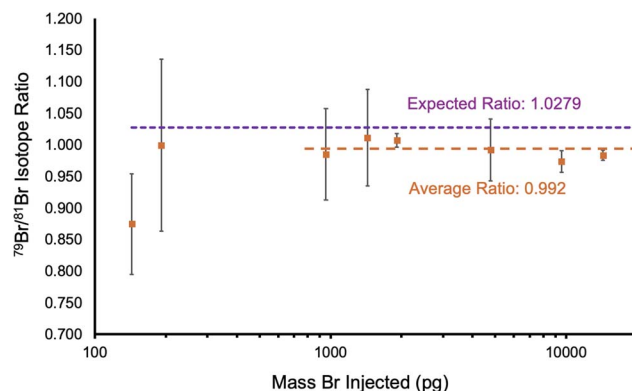
Fig. 6 Determined $^{79}Br/^{81}Br$ isotope ratios obtained for triplicate 20 μL injections across a bromine mass of 0.019 to 191.2 ng, with the accepted isotope ratio and the value determined from the concentrations above the determined LOQ presented.

more refined isotope ratio data acquisition protocol using the FTMS Booster including longer digitization transients and $n = 10$ determinations. These preliminary data points bode very well for future Br IR determinations at concentration levels that rival ICP-MS.

A key question moving forward into the realm of halogen determinations is the potential role of the counter ion (cation) identity on the responsivity of the halide. One could certainly imagine that there might be influences based on the strength of the ionic interactions and perhaps changes in plasma operation conditions based on the identity of the electrolytic cations. A preliminary assessment to this end was performed to gauge the method's versatility across various halogen salts. Initial testing focused on bromide anions from NaBr, KBr, and MgBr$_2$; two monocations and one dication. Across this range of compounds, the metal–bromine bond strengths vary from 297 kJ mol^{-1} for MgBr$_2$ to 383 kJ mol^{-1} for KBr.[48] To ensure that that same quantity of bromine was being evaluated, the molarities of the three solutions were set to achieve Br$^-$ concentrations of 10 μg mL^{-1}. Across three injections of each solution, the average values of the Br$^-$ responses varied by only 6%, relative; on the same level as the injection-to-injection variability. Thus, the cation type had no discernible impact on the method's ability to detect elemental bromide anions. This finding suggests perhaps a surprising robustness of the low temperature microplasma, as it remains unaffected by the cation composition of the salt. Far more extensive investigations into additional halogen salts, particularly those containing iodide, are required the validate the method's efficacy. Given their prevalence in environmental samples, studies of organohalides are also in order.

Conclusions

This study presents an initial evaluation of the potential of the LS-APGD-Orbitrap-MS system as a powerful tool for detecting multiple halogens in their elemental form while avoiding interferences common in other MS approaches and minimizing
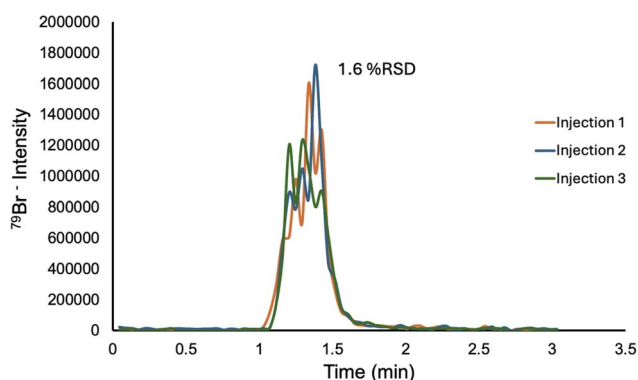

Fig. 5 Transient signals acquired from triplicate 20 μL injections of 2 ng Br in the form of NaBr for isotope ratio determinations, yielding a precision of 1.6% RSD for the integrated areas.

2630 | *J. Anal. At. Spectrom.*, 2025, **40**, 2625–2632

This journal is © The Royal Society of Chemistry 2025

the need for extensive sample preparation. Using this method at the optimized MS (CID value of 40 eV and HCD value of 20 eV) and plasma (0.5 mm electrode gap, solution flow rate of 60 μL min^{-1}, sheath gas flow rate of 600 mL min^{-1}, and a current of 60 mA) conditions allows for a limit of detection on the picogram level for both bromide and iodide anions without the use of specialized data acquisition methods. The system's precision in initial bromine isotope ratio determinations complements its already established promise in nuclear forensics and safeguarding efforts, where accuracy and reliability are paramount. The determination of bromine in the case of different salt (counter ion) forms suggests the method's robustness, with further testing certainly required on more diverse bromine and iodine salts required to scope out the range of applicability. Looking ahead, challenging applications such as the characterization of halogen elements in uranium ore concentrates will be a primary focus. While the mass resolution of the Orbitrap mass analyzer were not required in these studies, suggesting the potential use of lower-resolution platforms that still provide CID capabilities, more complex matrices may reveal the need for the resolution afforded by that format. Additionally, the scope of this technology will be expanded to include the detection of other halogen elements including fluorine and chlorine, in those instances, though, the 50 Da lower mass limit of the Orbitrap instrument eliminates the possibility of atomic halide detection, and so determinations in the molecular forms will be required.

Author contributions

Dehlia A. Lang: methodology, data curation, visualization, writing – original draft preparation; Cameron J. Stouffer: methodology; Joseph V. Goodwin: methodology; Benjamin T. Manard: supervision, reviewing, editing; R. Kenneth Marcus: conceptualization, supervision, writing – reviewing and editing.

Conflicts of interest

The authors declare that they have no known competing financial interests or personal relationships that could have appeared to influence the work reported in this paper.

Data availability

The data generated in the research described here is available from the corresponding author upon written request.

Acknowledgements

References

1 B. Schnetger and Y. Muramatsu, *Analyst*, 1996, **121**, 1627–1631.
2 K. Tagami, S. Uchida, I. Hirai, H. Tsukada and H. Takeda, *Anal. Chim. Acta*, 2006, **570**, 88–92.
3 A. L. G. Mendes, G. R. Bitencourt, G. D. Iop, S. R. Krzyzaniak, D. M. Souza and P. A. Mello, *Rev. Virtual Quim.*, 2023, **15**, 879–886.
4 D. Clases, R. Gonzalez de Vega, J. Parnell and J. Feldmann, *J. Anal. At. Spectrom.*, 2023, **38**, 1661–1667.
5 E. Keegan, M. Wallenius, K. Mayer, Z. Varga and G. Rasmussen, *Appl. Geochem.*, 2012, **27**, 1600–1609.
6 L. Xu, C. Luo, H. Ling, Y. Tang and H. Wen, *Int. J. Mass Spectrom.*, 2018, **432**, 52–58.
7 M. Martinez, G. J. Harry, E. N. Haynes, P.-I. D. Lin, E. Oken, M. K. Horton, R. O. Wright, M. Arora and C. Austin, *J. Anal. At. Spectrom.*, 2023, **38**, 303–314.
8 R. Gonzalez de Vega, A. Cameron, D. Clases, T. M. Dodgen, P. A. Doble and D. P. Bishop, *J. Chromatogr. A*, 2021, **1653**, 462423.
9 N. D. Fletcher, B. T. Manard, S. C. Metzger, B. W. Ticknor, D. A. Bostick and C. R. Hexel, *J. Radioanal. Nucl. Chem.*, 2020, **324**, 395–402.
10 S. Bürger, S. F. Boulyga, M. V. Peńkin, D. Bostick, S. Jovanovic, R. Lindvall, G. Rasmussen and L. Riciputi, *J. Radioanal. Nucl. Chem.*, 2014, **301**, 711–729.
11 P. A. Mello, J. S. Barin, F. A. Duarte, C. A. Bizzi, L. O. Diehl, E. I. Muller and E. M. M. Flores, *Anal. Bioanal. Chem.*, 2013, **405**, 7615–7642.
12 K.-e. Wang and S.-J. Jiang, *Anal. Sci.*, 2008, **24**, 509–514.
13 A. Earnshaw and N. N. Greenwood, *Chemistry of the Elements*, Butterworth-Heinemann, Oxford, 1997.
14 E. M. M. Flores, P. A. Mello, S. R. Krzyzaniak, V. H. Cauduro and R. S. Picoloto, *Rapid Commun. Mass Spectrom.*, 2020, **34**, e8727.
15 B. J. Riley, C. L. Beck, J. S. Evarts, S. Chong, A. M. Lines, H. M. Felmy, J. McFarlane, H. B. Andrews, S. A. Bryan, K. C. McHugh, H. S. Cunningham, R. M. Asmussen, J. A. Dhas, Z. Zhu, J. V. Crum, S. D. Shen, J. S. McCloy and Z. M. Heiden, *AIP Adv.*, 2024, **14**, 080701.
16 T. Van Acker, S. Theiner, E. Bolea-Fernandez, F. Vanhaecke and G. Koellensperger, *Nat. Rev. Methods Primers*, 2023, **3**, 52.
17 X. Bu, T. Wang and G. Hall, *J. Anal. At. Spectrom.*, 2003, **18**, 1443–1451.
18 C. D. Quarles, A. D. Toms, R. Smith, P. Sullivan, D. Bass and J. Leone, *Talanta Open*, 2020, **1**, 100002.
19 N. L. A. Jamari, J. F. Dohmann, A. Raab, E. M. Krupp and J. Feldmann, *J. Anal. At. Spectrom.*, 2017, **32**, 942–950.
20 R. K. Marcus, B. T. Manard and C. D. Quarles, *J. Anal. At. Spectrom.*, 2017, **32**, 704–716.
21 R. K. Marcus, C. D. Quarles Jr., C. J. Barinaga, A. J. Carado and D. W. Koppenaal, *Anal. Chem.*, 2011, **83**, 2425–2429.
22 D. W. Koppenaal and R. K. Marcus, *Appl. Spectrosc.*, 2023, **77**, 885–906.

This journal is © The Royal Society of Chemistry 2025

J. Anal. At. Spectrom., 2025, **40**, 2625–2632 | **2631**

23 L. X. Zhang, B. T. Manard, B. A. Powell and R. K. Marcus, *Anal. Chem.*, 2015, **87**, 7218–7225.

24 L. X. Zhang and R. K. Marcus, *J. Anal. At. Spectrom.*, 2016, **31**, 145–151.

25 T. J. Williams, J. R. Bills and R. K. Marcus, *J. Anal. At. Spectrom.*, 2020, **35**, 2475–2478.

26 E. H. Evans, in *Encyclopedia of Analytical Science*, ed. P. Worsfold, A. Townshend and C. Poole, Elsevier, Oxford, 2nd edn, 2005, pp. 229–237, DOI: **10.1016/B0-12-369397-7/00036-4**.

27 A. Montaser, *Inductively Coupled Plasma Mass Spectroscopy: Novel Instrumentation and Applications*, John Wiley & Sons, Inc., 2nd edn, 2020.

28 C. D. Quarles Jr, A. J. Carado, C. J. Barinaga, D. W. Koppenaal and R. K. Marcus, *Anal. Bioanal. Chem.*, 2012, **402**, 261–268.

29 E. D. Hoegg, S. Godin, J. Szpunar, R. Lobinski, D. W. Koppenaal and R. K. Marcus, *J. Anal. At. Spectrom.*, 2019, **34**, 1387–1395.

30 J. R. Bills, K. O. Nagornov, A. N. Kozhinov, T. J. Williams, Y. O. Tsybin and R. K. Marcus, *J. Am. Soc. Mass Spectrom.*, 2021, **32**, 1224–1236.

31 R. K. Marcus, *Chimia*, 2025, **79**, 60–65.

32 J. V. Goodwin, B. T. Manard, B. W. Ticknor, P. Cable-Dunlap and R. Kenneth Marcus, *Microchem. J.*, 2024, **196**, 109645.

33 E. D. Hoegg, S. Godin, J. Szpunar, R. Lobinski, D. W. Koppenaal and R. K. Marcus, *Anal. Chem.*, 2021, **93**, 11506–11514.

34 J. V. Goodwin, C. Masucci, D. Bleiner and R. K. Marcus, *J. Anal. At. Spectrom.*, 2024, **39**, 2353–2362.

35 J. V. Goodwin, B. T. Manard, B. W. Ticknor, P. Cable-Dunlap and R. K. Marcus, *Anal. Chem.*, 2023, **95**, 12131–12138.

36 J. V. Goodwin, B. T. Manard, B. W. Ticknor, P. Cable-Dunlap and R. K. Marcus, *J. Anal. At. Spectrom.*, 2022, **37**, 814–822.

37 E. D. Hoegg, C. J. Barinaga, G. J. Hager, G. L. Hart, D. W. Koppenaal and R. K. Marcus, *J. Am. Soc. Mass Spectrom.*, 2016, **27**, 1393–1403.

38 K. O. Nagornov, M. Zennegg, A. N. Kozhinov, Y. O. Tsybin and D. Bleiner, *J. Am. Soc. Mass Spectrom.*, 2020, **31**, 257–266.

39 Y. O. Tsybin, K. O. Nagornov and A. N. Kozhinov, in *Fundamentals and Applications of Fourier Transform Mass Spectrometry*, ed. B. Kanawati and P. Schmitt-Kopplin, Elsevier, 2019, pp. 113–132, DOI: **10.1016/B978-0-12-814013-0.00005-3**.

40 E. Denisov, E. Damoc and A. Makarov, *Int. J. Mass Spectrom.*, 2021, **466**, 116607.

41 J. V. Goodwin, B. T. Manard and R. K. Marcus, *Rapid Commun. Mass Spectrom.*, 2024, **38**, e9912.

42 T. J. Williams, E. D. Hoegg, J. R. Bills and R. K. Marcus, *Int. J. Mass Spectrom.*, 2021, **464**, 116572.

43 J. E. House and K. A. House, in *Descriptive Inorganic Chemistry*, ed. J. E. House and K. A. House, Academic Press, Amsterdam, 2nd edn, 2010, pp. 375–400, DOI: **10.1016/B978-0-12-088755-2.00016-1**.

44 S. Shrestha, J. V. Goodwin, B. T. Manard and R. K. Marcus, *Int. J. Mass Spectrom.*, 2025, **508**, 117385.

45 F. Gelman and A. Dybala-Defratyka, *Chemosphere*, 2020, **246**, 125746.

46 Y. Du, T. Ma, J. Yang, L. Liu, H. Shan, H. Cai, C. Liu and L. Chen, *Int. J. Mass Spectrom.*, 2013, **338**, 50–56.

47 *Bromine, U.S. Department of Energy Isotope Program*, **https://www.isotopes.gov**.

48 *Lange's Handbook of Chemistry*, ed. J. A. Dean, McGraw-Hill, New York, 1999.

2632 | *J. Anal. At. Spectrom.*, 2025, **40**, 2625–2632

This journal is © The Royal Society of Chemistry 2025